

---

# PDEexplain: Contextual Modeling of PDEs in the Wild

---

Ori Linial<sup>1</sup> Orly Avner<sup>2</sup> Dotan Di Castro<sup>2</sup>

## Abstract

We propose an explainable method for solving Partial Differential Equations by using a contextual scheme called *PDEexplain*. During the training phase, our method is fed with data collected from an operator-defined family of PDEs accompanied by the general form of this family. In the inference phase, a minimal sample collected from a phenomenon is provided, where the sample is related to the PDE family but not necessarily to the set of specific PDEs seen in the training phase. We show how our algorithm can predict the PDE solution for future timesteps. Moreover, our method provides an explainable form of the PDE, a trait that can assist in modelling phenomena based on data in physical sciences. To verify our method, we conduct extensive experimentation, examining its quality both in terms of prediction error and explainability.

## 1. Introduction

Many scientific fields use the language of Partial Differential Equations (PDEs; [Evans, 2010](#)) to describe the physical laws governing observed natural phenomena with spatio-temporal dynamics. Typically, a PDE system is derived from first principles and a mechanistic understanding of the problem after experimentation and data collection by domain experts of the field. Well-known examples for such systems include Navier-Stokes and Burgers' equations in fluid dynamics, Maxwell's equations for electromagnetic theory, and Schrödinger's equations for quantum mechanics. Solving a PDE model could provide users with crucial information on how a signal evolves over time and space, and could be used for both prediction and control tasks.

While solving PDEs holds great value, it might still be a difficult task in many cases (we refer the reader to [Zwillinger & Dobrushkin, 1998](#) for an extensive handbook for analytical methods). For many complex real-world phenomena, we

might only know some of the dynamics of the system. For example, an expert might tell us that a heat equation PDE has a specific functional form but we do not know the values of the diffusion and drift coefficient functions. In this paper we focus mainly on this case.

There are different ways of solving PDEs when data is available. In [Figure 1](#) we illustrate the spectrum of approaches to the problem of PDEs modeling and their solutions. The horizontal axis represents the amount of mechanistic knowledge required by each approach, i.e., how much prior knowledge we have on the source of the data in terms of the PDE structure. The approaches hovering above the axis are those that employ available data, while those below the axis only use mechanistic knowledge. We describe the different approaches in detail in [Section 4](#).

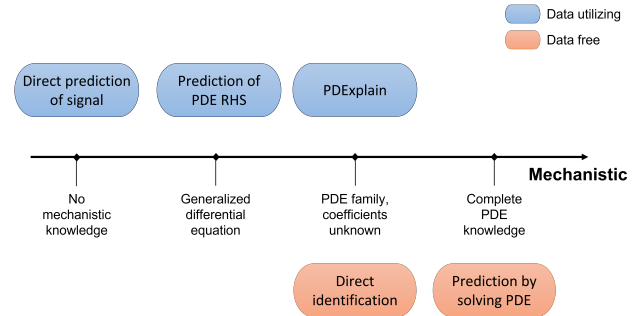


*Figure 1.* Mechanistic and data driven approaches to PDE modeling. The horizontal axis represents mechanistic knowledge and the vertical location of the approaches corresponds to the ability to utilize training data.

The current process of solving PDEs over space and time is by using numerical differentiation and integration schemes. However, numerical methods may require significant computational resources, making the PDE solving task feasible only for low-complexity problems, e.g., a small number of equations. An alternative wide-used approach is finding simplified models that are based on certain assumptions and can roughly describe the problem's dynamics. A known example for such a model are the Reynolds-averaged Navier-Stokes equations ([Reynolds, 1895](#)). Building simplified models is considered a highly non-trivial task that requires special expertise, and might still not represent the

<sup>1</sup>Technion - Israel Institute of Technology, Haifa, Israel <sup>2</sup>Bosch Center for Artificial Intelligence, Haifa, Israel. Correspondence to: Ori Linial <linial04@gmail.com>.

phenomenon to a satisfactory accuracy.

In recent years, with the rise of Deep Learning (DL; LeCun et al., 2015), novel methods for solving numerically-challenging PDEs were devised. These methods have become especially useful thanks to the rapid development of sensors and computational power, enabling the collection of large amounts of multidimensional data related to a specific phenomenon. In general, DL based approaches consume the observed data and learn a black-box model of the given problem that can then be used to provide predictions for the dynamics. While this set of solutions has been shown to perform successfully on many tasks, it still suffers from two crucial drawbacks: (1) It offers no explainability as to why the predictions were made, and (2) it usually performs very poorly when extrapolating to unseen data.

In this paper, we offer a new hybrid modelling (Kurz et al., 2022) approach that can benefit from both worlds: it can use the vast amount of data collected on one hand, and utilize the partially known PDEs describing the natural phenomena observed on the other hand. In addition, it can learn several contexts, therefore, employing the generalization capabilities of DL models, enabling a zero-shot learning (Palatucci et al., 2009). Specifically, our model is given a general functional form of the PDE (i.e., which derivatives are used and what the form of the coefficient functions is), consumes the observed data, and outputs the unknown coefficient functions. Then, we can then use off-the-shelf PDE solvers (e.g., PyPDE<sup>1</sup>) to solve and create predictions of the given task forward in time for any horizon.

Another key feature of our approach is that it consumes the spatio-temporal input signals required for training in an unsupervised manner, namely the coefficient functions that created the signals in the train set are unknown. This is achieved by combining an autoencoder (AE; Kramer, 1991) architecture with a loss defined using the functional form of the PDE. As a result of this feature, large amounts of training data for our algorithm can be easily acquired. Moreover, our ability to generalize to data corresponding to a PDE whose coefficients did not appear in the train set, enables the use of synthetic data for training. In addition, although our approach is intended to work when the PDE functional form is known, it is not limited to that scenario only. In cases where we are given a misspecified model (when experts provide a surrogate model for instance), our model can eliminate some of the discrepancies in the extra function that is not a coefficient of one of the derivatives (the  $p_0(x, t, f)$  function in Eq. (1))

Finally, our approach may also be feasible for tremendously computationally intensive problems like weather prediction (Kang et al., 2021) or simulating waves (Lisitsa et al., 2012).

In such cases the PDEs are known but most researchers do not have access to High Performance Computing so a hybrid model as we propose might be handy.

We summarize our contribution as follows:

1. Harnessing the information contained in large datasets belonging to a phenomenon which is related to a PDE functional family in an unsupervised manner. Specifically, we propose a regression based method for doing that.
2. Proposing a DL encoding scheme for the context conveyed in such datasets, enabling generalization for prediction of unseen samples based on minimal input, similarly to zero-shot learning.
3. Extensive experimentation with the proposed scheme, examining the effect of context and train set size, along with a comparison to different previous methods.

The paper is organized as follows. In Section 2 we review related work. In Section 3 we present the proposed method and in Section 4 we provide experiments to support our method. Section 5 completes the paper with conclusions and future directions.

## 2. Related Work

Creating a neural-network based model for approximating the solution of a PDE has been studied in many related works over the years, and dates back more than a decade (Lagaris et al., 1998). We divide deep learning based existing work by their ability to incorporate mechanistic knowledge in their models, and by the type of information that can be extracted from using them. An additional distinction between different approaches is their ability to handle datasets originating from different contexts. From a PDE perspective, a different context could refer to having data signals generated with different coefficients functions ( $p_i$  in Eq. (1)). In many real-world applications, obtaining observed datasets originating from a single context is highly infeasible. For example, in cardiac electrophysiology (Neic et al., 2017), patients differ in cardiac parameters like resistance and capacitance, thus representing different contexts. In fluid dynamics, the topography of the underwater terrain (bathymetry) differs from one sample to another (Hajduk et al., 2020). A benchmark and dataset work (PDEBench) that provides a large amount of datasets governed by known PDEs has been released recently (Takamoto et al., 2022), but each of the datasets provided by it is generated from a single constant function (i.e., all data samples have the same context).

The first line of work is purely data-driven based methods. These models come in handy especially when we observe a

<sup>1</sup><https://pypde.readthedocs.io/en/latest/>

spatio-temporal phenomenon, but either don't have enough knowledge of the underlying PDE dynamics that generated the observed signal, or the known equations are too complicated to solve numerically (as explained thoroughly by Wang & Yu, 2021). Recent advances demonstrate successful prediction results that are both fast to compute (compared to numerically solving a PDE), and also shown to provide decent predictions even for PDEs with very high dimensions (Brandstetter et al., 2022; Li et al., 2020; Han et al., 2018; Lu et al., 2019). However, the downside of this approach is not being able to infer the PDE coefficients, which may hold valuable information and explanations as to why the model formed its predictions.

The second type of data-driven methods are approaches that can utilize PDE forms known beforehand to some extent. Works that adopt this approach can usually utilize the given mechanistic knowledge and provide reliable predictions, ability to generalize to unseen data, and even, in some cases, reveal part of the underlying PDE coefficient functions. However, their main limitation is that they assume the entire training dataset is generated by a single coefficient function and only differ in the initial conditions (or possibly boundary conditions). PDE-NET (Long et al., 2018), its followup PDE-NET2 (Long et al., 2019), DISCOVER (Du et al., 2022), PINO (Li et al., 2021) and sparse-optimization methods (Schaeffer, 2017; Rudy et al., 2017) (expanding the idea originally presented on ODEs in (Brunton et al., 2016; Champion et al., 2019)), are not given the PDE system, but instead aim to learn some representation of the underlying PDE as a linear combination of base functions and derivatives of the PDE state. PINN (Raissi et al., 2019) and NeuralPDE (Zubov et al., 2021) assume full knowledge of the underlying PDE including the its coefficients, and aim to replace the numerical PDE solver by a fast and reliable model. They also provide a scheme for finding the PDE parameters as scalars, but assume the entire dataset is generated by a single coefficient value, while we assume each sample is generated with different coefficient values and could be functions of time, space and state (as described in Eq. (1)). Similarly, Learning-informed PDEs (Dong et al., 2022; Aarset et al., 2022) suggest a method that assumes full knowledge of the PDE derivatives and their coefficient functions, and infers the free coefficient function (namely  $p_0(x, t, u)$  in Eq. (1)).

The last line of work, and closer in spirit to ours, includes context-aware methods that assume some mechanistic knowledge, with each sample in the train set generated by different PDE coefficients (we also refer to this concept as having different context) and initial conditions. CoDA (Kirchmeyer et al., 2022) provides an ability to form predictions of signals with unseen contexts, but does not directly identify the PDE parameters. GOKU (Linial et al., 2021) and ALPS (Yang et al., 2022) provide context-aware infer-

ence of signals with ODE dynamics, when the observed signals are not the ODE variables directly.

### 3. Method

The data we handle is a set of spatio-temporal signals, generated by an underlying PDE with partial knowledge of its form and its boundary conditions. The coefficient functions determining the exact PDE are unknown and may be different for each collection of data. Our goal is to estimate these coefficient functions and provide reliable predictions of the future time steps of the observed phenomenon. The proposed method comprises three subsequent parts: (1) Creating a compact representation of the given signal, (2) estimating the PDE coefficients, and (3) solving the PDE using the acquired knowledge. Although the proposed method may be generalized to other PDE types, for ease of exposition, we focus on parabolic PDEs in this section.

#### 3.1. Problem Formulation

We now define the problem at hand formally. Let  $u(x, t)$  denote a signal with spatial support  $x \in [0, L]$  and temporal support  $t \in [0, T]$ . We refer to this as the *complete* signal. Next, we define  $u^c(x, t)$  to be a partial input signal, a *patch*, where its support is  $x \in [0, L]$ ,  $t \in [0, t_0]$ , and where  $0 < t_0 < T$ . The superscript  $c$  stands for context.

We assume the signal  $u(x, t)$  is the solution of a  $k$ -order PDE of the general form

$$\frac{\partial u}{\partial t} = \sum_{l=1}^k p_l(x, t, u) \frac{\partial u^l}{\partial x^l} + p_0(x, t, u), \quad (1)$$

where we denote the vector of coefficient functions by  $p = (p_0, \dots, p_k)$ . We adopt the notation of Wang & Yu (2021) and refer to a family of PDEs characterized by a vector  $p$  as an operator  $F(p, u)$ , where solving  $F(p, u) = 0$  yields solutions of the PDE.

The problem we solve is as follows: given a patch  $u^c(x, t)$ , that solves a PDE of a *known* operator  $F$  with an *unknown* coefficient vector  $p$ , we would like to (a) estimate the coefficient vector  $\hat{p}$  and (b) predict the complete signal  $\hat{u}(x, t)$  for  $0 \leq t \leq T$ .

Our solution is a concatenation of two neural networks, which we call *PDEexplain*. Its input is a patch, and its output is a vector  $\hat{p}$ . We feed this vector into an off-the-shelf PDE solver together with the operator  $F(p, u)$  to obtain the predicted signal  $\hat{u}(x, t)$ .

The partial derivatives are estimated using standard numerical schemes for each point in the patch. We choose discretization parameters  $\Delta x$  for the spatial axis and  $\Delta t$  for the temporal axis where we solve the PDE numerically on the grid points  $\{(i\Delta x, j\Delta t)\}_{i=0, j=0}^{N_x, N_t}$  with  $L = N_x\Delta x$  and

$T = N_t \Delta t$ . Let us denote the numerical solution with  $\hat{u}_{i,j}$ . We use the *forward-time central-space* scheme, so a second order scheme from (1) would be

$$\begin{aligned} \frac{\hat{u}_{i,j+1} - \hat{u}_{i,j}}{\Delta t} &= p_2(i, j, u(i, j)) \frac{\hat{u}_{i+1,j} - 2\hat{u}_{i,j} + \hat{u}_{i-1,j}}{\Delta x^2} \\ &+ p_1(i, j, u(i, j)) \frac{\hat{u}_{i+1,j} - \hat{u}_{i-1,j}}{2\Delta x} \\ &+ p_0(i, j, u(i, j)) \end{aligned} \quad (2)$$

For ease of exposition we omit some details and refer the reader to (Strikwerda, 2004) for a complete explanation.

### 3.2. PDExplain Inference

We begin by outlining our inference process, presented in Fig. 2. The input to this process is a patch  $u^c(x, t)$ , where  $x \in [0, L]$ ,  $t \in [0, t_0]$  and an operator  $F$  (e.g., the one introduced in Eq. (1) for  $k = 2$ ). The patch is fed into the PDExplain component, which generates the estimated coefficients  $\hat{p}$ , in the example,  $\hat{p} = (\hat{a}, \hat{b}, \hat{c})$ . The PDE solver then uses this estimate to predict the complete signal,  $\hat{u}(x, t)$ ,  $x \in [0, L]$ ,  $t \in [t_0, T]$ . An important feature of our approach is the explicit prediction of the coefficient functions, which contributes to the explainability of the solution.

The patch  $u^c(x, t)$  is a partial signal that serves as an initial condition for the prediction and also represents the dynamics of the signal for estimating the PDE coefficients. In the sequel we refer to it as ‘‘context’’. The ratio of the context is denoted by  $\rho$ , such that  $t_0 = \rho T$ , and is a hyper-parameter of our algorithm. We discuss the effect of context size in Section 4.1.2.

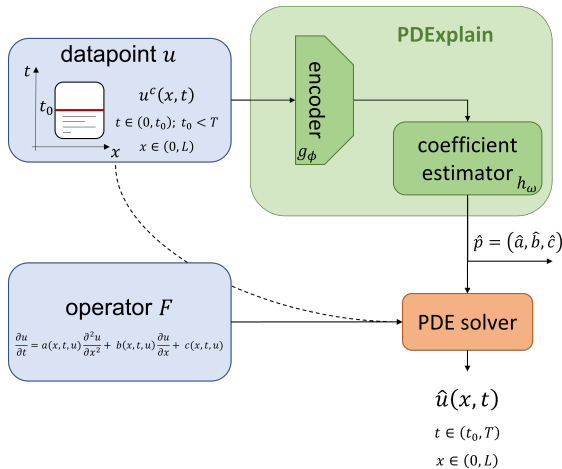


Figure 2. Inference process. Dashed line is initial condition, supplied to the PDE solver together with the estimated coefficients and operator  $F$ .

### 3.3. PDExplain Training

The training process is presented in Fig. 3. Its input is a dataset  $U$  that consists of  $N$  complete signals  $\{u_i(x, t)\}_{i=1}^N$  which are solutions of  $N$  PDEs that share an operator  $F$  but have unique coefficient vectors  $\{p_i\}_{i=1}^N$ . The support of the signals is  $x \in [0, L]$  and  $t \in [0, T]$ . The loss we minimize is a weighted sum of two components: (i) the functional loss as defined in Eq. (4) and (ii) the autoencoder reconstruction loss (AE; Hinton & Salakhutdinov, 2006), which is defined in Eq. (3).

The PDExplain scheme is composed of two components: (1) an encoder and (2) a coefficient estimator, both of which proved essential over the course of our work. The encoder’s goal is to capture the dynamics driving the signal  $u_i$ , thus creating a compact representation for the coefficient estimator. The encoder is trained on patches  $u_i^c$  randomly taken from signals  $u_i$  belonging to the train set. Each patch is of size  $t_0 \times L$ .

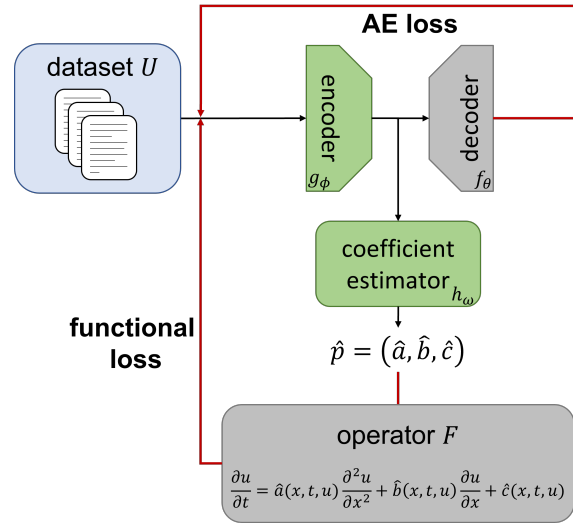


Figure 3. Training process.

The encoder loss is the standard autoencoder reconstruction loss (Hinton & Salakhutdinov, 2006), namely the objective is

$$\min_{\theta, \phi} \mathcal{L}_{\text{AE}} = \min_{\theta, \phi} \sum_{i=1}^N \text{loss}(u_i^c - f_{\theta}(g_{\phi}(u_i^c))), \quad (3)$$

where  $f_{\theta}$  is the decoder,  $g_{\phi}$  is the encoder and  $\text{loss}(\cdot, \cdot)$  is a standard loss function (e.g.,  $L^2$  loss).

The second component is the coefficient estimator, whose input is the encoded context. The estimated coefficients output by this component, together with the operator  $F$ ,

**Algorithm 1** PDEexplain inference scheme

**Input:** patch  $u^c(x, t)$ , operator  $F$ , trained networks: decoder  $g_\phi$ , coefficient estimator  $h_\omega$   
 $\hat{p} \leftarrow h_\omega(g_\phi(u^c))$   
 $\hat{u} \leftarrow \text{PDE\_solve}(F, \hat{p}, u^c(x, t = t_0))$   
 return  $\hat{u}, \hat{p}$

form the functional objective:

$$\min_{\omega} \mathcal{L}_{\text{coef}} = \min_{\omega} \sum_{i=1}^N \|F(\hat{p}_\omega, u_i^c)\|^2, \quad (4)$$

where  $\omega$  represents the parameters of the coefficient estimator network, and  $\hat{p}$  is the estimator of  $p$ , acquired by applying the network  $h_\omega$  to the output of the encoder.

The two components are trained simultaneously, and the total loss is a weighted sum of the losses in Eq. (3) and Eq. (4)

$$\mathcal{L} = \alpha \cdot \mathcal{L}_{\text{AE}} + (1 - \alpha) \cdot \mathcal{L}_{\text{coef}}, \quad (5)$$

where  $\alpha \in (0, 1)$  is a hyper-parameter.

Both networks are simple fully connected networks. Naturally, they can be further optimized to improve performance, but the results presented in Section 4 attest to the robustness of our approach. A key feature of the proposed method is lack of supervision, in the sense that unlike many previous approaches, the coefficient values of the PDEs represented in the train set are *unknown even at training time*. The algorithm succeeds in its task by combining an autoencoder architecture with the mechanistic knowledge contained in the PDE functional form. We experimented with removing the decoder and training the networks using the functional loss alone, but results proved to be poor.

To summarize this section, we present the inference scheme in Algorithm 1, and the full training algorithm in Algorithm 2.

## 4. Experiments

We devote this section to two types of analyses: (a) a comparison of our approach to other solutions, and (b) an analysis of our approach in different regimes.

The dataset we use includes 10,000 samples of size  $100 \times 40[t \text{ points} \times x \text{ points}]$ , where each sample is a signal generated from a PDE with different coefficients. We stress the fact that the test set contains signals generated by PDEs with coefficient vectors that *do not* appear in the training data, resulting in a zero-shot prediction problem. More information about dataset creation can be found in the appendix.

In our experiments we implement three algorithms, in addition to our proposed PDEexplain, corresponding to the

**Algorithm 2** Algorithm for training PDEexplain

**Input:** dataset  $U$ , operator  $F$ , context ratio  $\rho$ , loss weight  $\alpha$ , number of epochs  $N_e$   
**Init:** random weights in encoder  $g_\phi$ , decoder  $f_\theta$ , coefficient estimator  $h_\omega$   
**for** epoch in  $N_e$  **do**  
 $\mathcal{L} \leftarrow 0$   
 $U_N^c \leftarrow N$  random patches, one from each  $u_i \in U$   
**for**  $u_i^c$  in  $U_N^c$  **do**  
 $\hat{p}_i \leftarrow h_\omega(g_\phi(u_i^c))$   
 $\mathcal{L}_{\text{AE}} \leftarrow (u_i^c - f_\theta(g_\phi(u_i^c)))^2$   
 $\mathcal{L}_{\text{coef}} \leftarrow \|F(\hat{p}_i, u_i^c)\|^2$   
 $\mathcal{L} \leftarrow \mathcal{L} + \alpha \cdot \mathcal{L}_{\text{AE}} + (1 - \alpha) \cdot \mathcal{L}_{\text{coef}}$   
**end for**  
 $\phi, \theta, \omega \leftarrow \arg \min \mathcal{L}$   
**end for**

Table 1. Characteristics of the implemented algorithms.

Approach	Mechanistic knowledge	Training data	Explainability
No PDE	-	+	-
PDE RHS	-	+	-
DI	+	-	+
PDEexplain	+	+	+

different approaches presented in Figure 1. For the sake of fair comparison, all of the data utilizing approaches include a trainable encoder, similar to the one introduced in Section 3.3. The algorithms are:

- “No PDE”: Direct prediction of the signal  $\hat{u}(x, t)$ , given the partial signal (patch)  $u^c(x, t)$  and an encoding of it, learned from training data. No use of mechanistic knowledge.
- “DI”: Direct identification of the PDE coefficients from the partial signal  $u^c(x, t)$  using a maximum likelihood approach, followed by solving the resulting PDE to predict the signal. Assumes PDE family is known, parameters unknown. No use of training data.
- “PDE-RHS”: Prediction of the underlying PDE’s right-hand-side based on the partial signal (patch)  $u^c(x, t)$  and an encoding of it, followed by solving the resulting PDE to predict the signal. This an approach that combines training data with minimal mechanistic knowledge, similar to that suggested by Chen et al. (2018).

We summarize the different approaches in Table 1, adding the feature of explainability, available in schemes that explicitly estimate PDE coefficients.

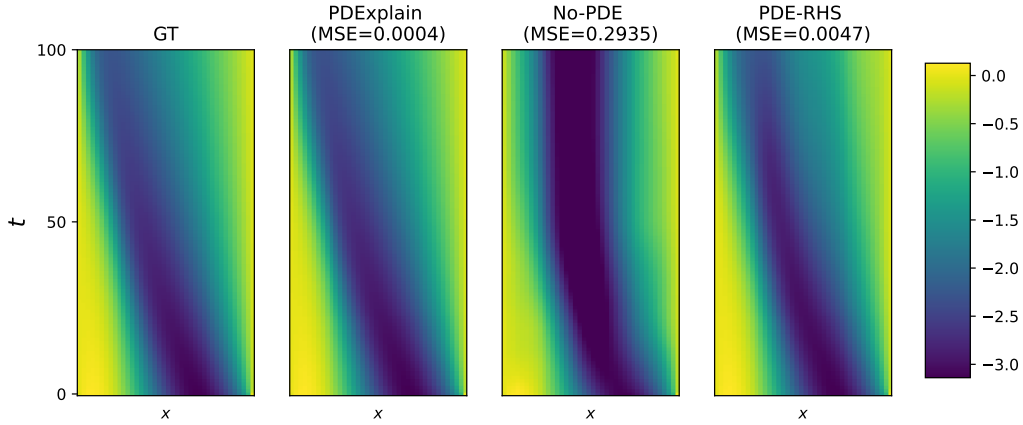


Figure 4. A solution of the Burgers' equation (prediction MSE appears in the title). The left panel displays the ground truth (GT), next to it the error-minimizing PDExplain prediction. No-PDE suffers from the largest error, which can be explained by its total lack of mechanistic knowledge. PDE-RHS achieves a relatively low MSE, but the quality of its prediction decreases over time.

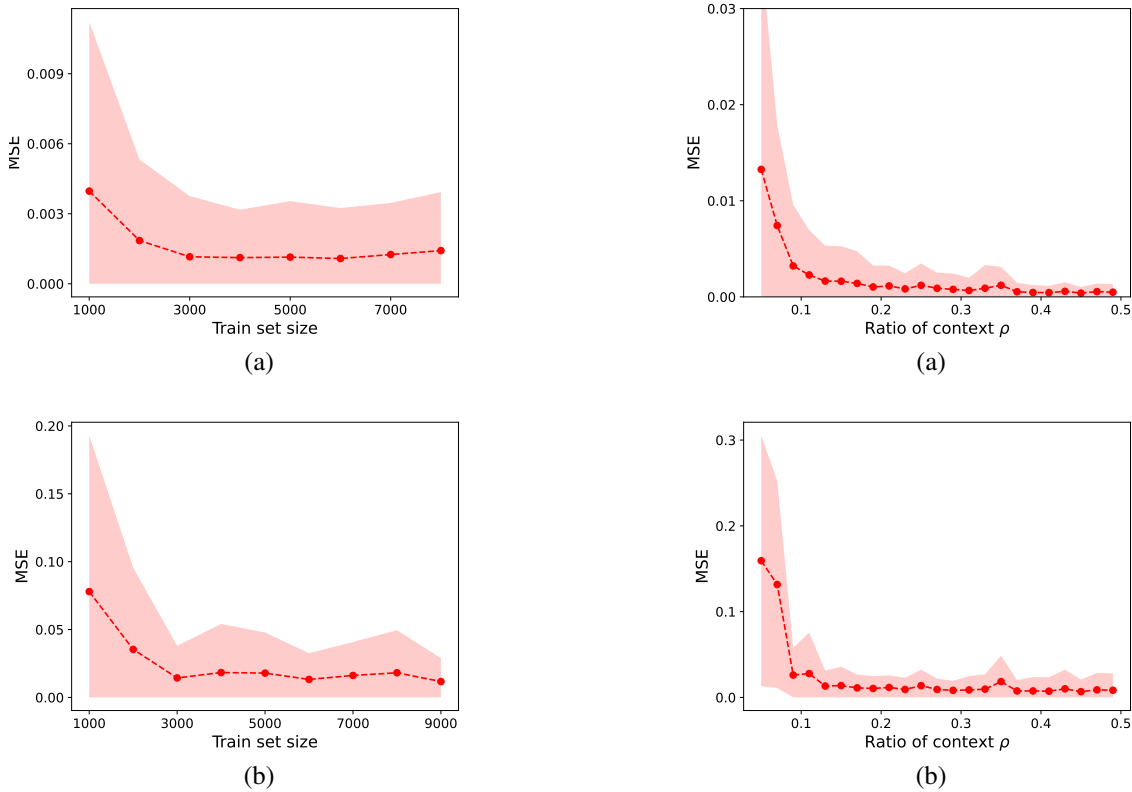


Figure 5. Constant coefficients PDE: (a) Prediction error of signal vs. train set size and (b) estimation error of parameter values vs. train set size. The error is calculated on a test set of 1000 samples.

Figure 6. Constant coefficients PDE: (a) Prediction error vs.  $\rho$  and (b) estimation error of parameter values error vs.  $\rho$ . The error is calculated on a test set of 1000 samples.

#### 4.1. Second Order PDE with Constant Coefficients

The first family of PDEs used for our experiments is:

$$\frac{\partial u}{\partial t} = a \frac{\partial^2 u}{\partial x^2} + b \frac{\partial u}{\partial x} + c, \tag{6}$$

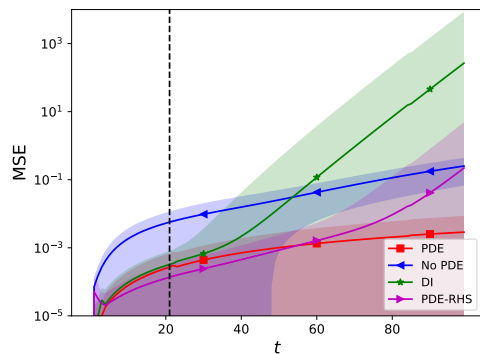


Figure 7. Prediction error as prediction horizon increases, for different approaches, PDE with constant coefficients. PDExplain, in red, is our approach. No PDE, in blue, learns an encoding for the training data and applies a purely data-driven prediction. DI, in green, corresponds to direct identification of the PDE coefficients from the datapoint, followed by solving the PDE (no training). The last approach, PDE-RHS, learns an encoding for the training data and predicts the right-hand-side of an equation which is then solved to yield an estimate of the signal. The dashed vertical line is the value of the context ratio used for this experiment (fixed for all approaches),  $\rho = 0.21$ .

where  $p = (a, b, c)$  are constants. Figure 7 demonstrates the clear advantage of our approach, which becomes increasingly larger as the prediction horizon increases (note the logarithmic scale of the vertical axis, representing the MSE of prediction). Since PDExplain harnesses both mechanistic knowledge and training data, it is able to predict the signal  $\hat{u}(x, t)$  several timesteps ahead, while keeping the error to a minimum. Next, we analyze the two parameters that characterize the PDExplain algorithm: train set size and context ratio.

#### 4.1.1. TRAIN SET SIZE

The train set size corresponds to  $N$ , the number of samples in dataset  $U$  of Algorithm 1. Figure 5 presents the decrease in the prediction and parameters error as we increase the train set size. This attests to the generalization achieved by the PDExplain architecture: as the train set grows and includes more samples with different values of coefficients, the ability to accurately estimate a new sample’s parameters and predict its rollout improves. In this set of experiments, 3,000 samples are generally enough to achieve a minimal error rate.

#### 4.1.2. CONTEXT RATIO

Another hyper-parameter of our system is the context ratio. Figure 6 presents the results of an experiment in which we vary its value as defined in Section 3.3. Simply put, as the context size increases, PDExplain encodes more informa-

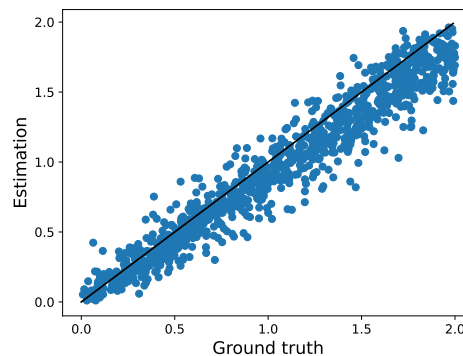


Figure 8. Constant coefficients PDE: estimated value of the  $\partial^2 u / \partial x^2$  coefficient vs. ground truth, for entire test set ( $R^2 = 0.93$ ).

tion regarding the input signal’s dynamics, thus the improvement in signal and parameter value prediction. The error decreases rather quickly, and a context ratio of 0.15 – 0.2 suffices for reaching a very low error, as is evident from the plots.

The last result for this set of experiments appears in Figure 8. Here, we plot the estimated value of parameter  $a$  of Eq. (6), against its true value. The plot and the high value of  $R^2$  demonstrate the low variance of our prediction, with a strong concentration of values along the  $y = x$  line.

## 4.2. Burgers’ equation

Another family of PDEs we experiment with is the quasi-linear Burgers’ equation, whose general form is

$$\frac{\partial u}{\partial t} = a \frac{\partial^2 u}{\partial x^2} + b(u) \frac{\partial u}{\partial x}, \quad (7)$$

where  $b(x, t, u) = -u$ , as presented in (Bateman, 1915). We note that this equation is quasi-linear since its drift coefficient  $b(x, t, u)$  depends on the solution  $u$  itself.

The dataset for our experiments consists of signals with different values of  $a$  and the same  $b(u) = -u$ , both unknown to the algorithm a priori. We begin with a demonstration of a signal  $u(x, t)$  and its prediction  $\hat{u}(x, t)$  in Figure 4. As can be seen both visually and from the value of the MSE (in each panel’s title), our approach yields a prediction that stays closest to the ground truth (GT), even as time advances and the prediction horizon increases.

Figure 9 displays a comparison between the different approaches to our problem. As before, the vertical axis of the plot is logarithmic, and the advantage of PDExplain over other approaches increases with the prediction horizon. The direct identification (DI) approach could not be applied to this family of PDEs, since it does not support coefficients

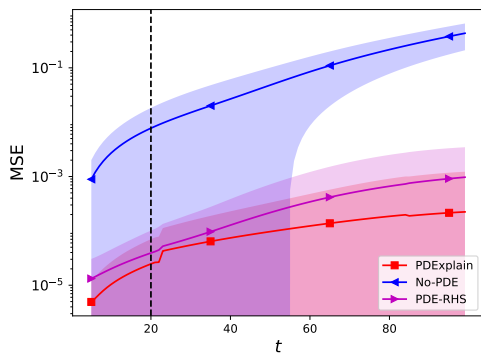


Figure 9. Prediction error as prediction horizon increases, for different approaches, Burgers’ PDE. PDExplain, in red, is our approach. No PDE, in blue, learns an encoding for the training data and applies a purely data-driven prediction. The last approach, PDE-RHS, learns an encoding for the training data and predicts the right-hand-side of an equation which is then solved to yield an estimate of the signal. The dashed vertical line is the value of the context ratio used for this experiment (fixed for all approaches),  $\rho = 0.2$ . The DI approach cannot be applied to equations with non-constant coefficients and is therefore omitted from the comparison.

that are functions, only constants.

In Figure 10 we focus on the ability to accurately predict coefficient functions with spatio-temporal dynamics, specifically in this case - the coefficient  $b(x, t, u)$  of Eq. (7). The different panels corresponds to different points in time, showing that the coefficient estimator tracks the temporal evolution successfully.

Table 2. Results summary for both the coefficient identification and signals prediction task, on two experiments: constant coefficients equation and Burgers’ equation. In both experiments we used  $\rho = 0.2$ , and report the MSE error. DI baseline in the constant coefficient experiment completely failed in predicting one of the test signals, so that measurement was omitted from the calculation to have a fair comparison.

METHOD	PARAMETERS MSE	PREDICTION MSE
CONSTANT PDE COEFFICIENTS		
PDEXPLAIN	$0.0116 \pm 0.014$	$0.0014 \pm 0.003$
DI	$0.0097 \pm 0.022$	$0.0067^* \pm 0.161$
NO-PDE	N/A	$0.0720 \pm 0.051$
PDE-RHS	N/A	$0.0174 \pm 0.326$
BURGERS’ PDE		
PDEXPLAIN	$0.0147 \pm 0.0188$	$0.0001 \pm 0.0004$
DI	N/A	N/A
NO-PDE	N/A	$0.1303 \pm 0.0839$
PDE-RHS	N/A	$0.0004 \pm 0.0010$

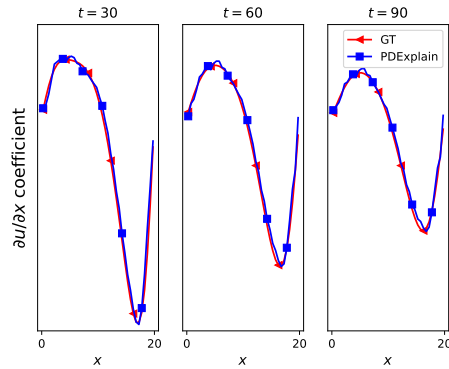


Figure 10. Estimation of the coefficient function  $b(x, t, u)$  of the Burgers’ equation, presented in Eq. (7). PDExplain manages to accurately estimate the spatio-temporal dynamics of the coefficient, based on a context ratio of  $\rho = 0.2$ .

## 5. Conclusion

In this work we introduce a new hybrid modelling approach, combining mechanistic knowledge with data. The knowledge we assume is in the form of a PDE family, without specific parameter values, typically supplied by field experts. The dataset we rely on is readily available in physical modelling problems, as it is simply a collection of spatio-temporal signals belonging to the same PDE family, with different parameters. Unlike other schemes, we do not require knowledge of the parameters of the PDE generating our train data.

We conduct extensive experiments, comparing our scheme to other solutions and testing its performance in different regimes. It achieves good results in the zero-shot learning problem, and is robust to different values of hyper-parameters.

Future directions we would like to pursue include adding support in our code for signals of higher spatial dimensions, together with a straightforward extension to handle signals with missing datapoints.

An interesting experiment we would like to conduct concerns handling “out of distribution” signals - generated by parameters beyond the support of the dataset, and the robustness of predicting such signals. Another question that comes to mind is whether including multiple signals generated by the same parameters has an effect on quality of results, similar to or different from that of the context ratio. Finally, we are eager to apply PDExplain to a real life problem like the ones mentioned in Section 2.



## References

- Aarset, C., Holler, M., and Nguyen, T. T. N. Learning-informed parameter identification in nonlinear time-dependent pdes. *arXiv preprint arXiv:2202.10915*, 2022.
- Bateman, H. Some recent researches on the motion of fluids. *Monthly Weather Review*, 43(4):163–170, 1915.
- Brandstetter, J., Worrall, D., and Welling, M. Message passing neural pde solvers. *arXiv preprint arXiv:2202.03376*, 2022.
- Brunton, S. L., Proctor, J. L., and Kutz, J. N. Discovering governing equations from data by sparse identification of nonlinear dynamical systems. *Proceedings of the national academy of sciences*, 113(15):3932–3937, 2016.
- Champion, K., Lusch, B., Kutz, J. N., and Brunton, S. L. Data-driven discovery of coordinates and governing equations. *Proceedings of the National Academy of Sciences*, 116(45):22445–22451, 2019.
- Chen, R. T., Rubanova, Y., Bettencourt, J., and Duvenaud, D. K. Neural ordinary differential equations. *Advances in neural information processing systems*, 31, 2018.
- Dong, G., Hintermüller, M., and Papafitsoros, K. Optimization with learning-informed differential equation constraints and its applications. *ESAIM: Control, Optimisation and Calculus of Variations*, 28:3, 2022.
- Du, M., Chen, Y., and Zhang, D. Discover: Deep identification of symbolic open-form pdes via enhanced reinforcement-learning. *arXiv preprint arXiv:2210.02181*, 2022.
- Evans, L. C. *Partial differential equations*, volume 19. American Mathematical Soc., 2010.
- Hajduk, H., Kuzmin, D., and Aizinger, V. *Bathymetry Reconstruction Using Inverse Shallow Water Models: Finite Element Discretization and Regularization*. Springer, 2020.
- Han, J., Jentzen, A., and E, W. Solving high-dimensional partial differential equations using deep learning. *Proceedings of the National Academy of Sciences*, 115(34):8505–8510, 2018.
- Hinton, G. E. and Salakhutdinov, R. R. Reducing the dimensionality of data with neural networks. *science*, 313(5786):504–507, 2006.
- Kang, J.-S., Myung, H., and Yuk, J.-H. Examination of computational performance and potential applications of a global numerical weather prediction model mpas using kisti supercomputer nurion. *Journal of Marine Science and Engineering*, 9(10):1147, 2021.
- Kirchmeyer, M., Yin, Y., Donà, J., Baskiotis, N., Rakotomamonjy, A., and Gallinari, P. Generalizing to new physical systems via context-informed dynamics model. *arXiv preprint arXiv:2202.01889*, 2022.
- Kramer, M. A. Nonlinear principal component analysis using autoassociative neural networks. *AIChE journal*, 37(2):233–243, 1991.
- Kurz, S., De Gersem, H., Galetzka, A., Klaedtke, A., Liebsch, M., Loukrezis, D., Russenschuck, S., and Schmidt, M. Hybrid modeling: towards the next level of scientific computing in engineering. *Journal of Mathematics in Industry*, 12(1):1–12, 2022.
- Lagaris, I. E., Likas, A., and Fotiadis, D. I. Artificial neural networks for solving ordinary and partial differential equations. *IEEE transactions on neural networks*, 9(5):987–1000, 1998.
- LeCun, Y., Bengio, Y., and Hinton, G. Deep learning. *nature*, 2015.
- Li, Z., Kovachki, N., Azizzadenesheli, K., Liu, B., Bhattacharya, K., Stuart, A., and Anandkumar, A. Fourier neural operator for parametric partial differential equations. *arXiv preprint arXiv:2010.08895*, 2020.
- Li, Z., Zheng, H., Kovachki, N., Jin, D., Chen, H., Liu, B., Azizzadenesheli, K., and Anandkumar, A. Physics-informed neural operator for learning partial differential equations. *arXiv preprint arXiv:2111.03794*, 2021.
- Linial, O., Ravid, N., Eytan, D., and Shalit, U. Generative ode modeling with known unknowns. In *Proceedings of the Conference on Health, Inference, and Learning*, pp. 79–94, 2021.
- Lisitsa, V., Reshetova, G., and Tcheverda, V. Finite-difference algorithm with local time-space grid refinement for simulation of waves. *Computational geosciences*, 16(1):39–54, 2012.
- Long, Z., Lu, Y., Ma, X., and Dong, B. Pde-net: Learning pdes from data. In *International Conference on Machine Learning*, pp. 3208–3216. PMLR, 2018.
- Long, Z., Lu, Y., and Dong, B. Pde-net 2.0: Learning pdes from data with a numeric-symbolic hybrid deep network. *Journal of Computational Physics*, 399:108925, 2019.
- Lu, L., Jin, P., and Karniadakis, G. E. DeepONet: Learning nonlinear operators for identifying differential equations based on the universal approximation theorem of operators. *arXiv preprint arXiv:1910.03193*, 2019.
- Neic, A., Campos, F. O., Prassl, A. J., Niederer, S. A., Bishop, M. J., Vigmond, E. J., and Plank, G. Efficient

- computation of electrograms and eegs in human whole heart simulations using a reaction-eikonal model. *Journal of computational physics*, 346:191–211, 2017.
- Palatucci, M., Pomerleau, D., Hinton, G. E., and Mitchell, T. M. Zero-shot learning with semantic output codes. *Advances in neural information processing systems*, 22, 2009.
- Raissi, M., Perdikaris, P., and Karniadakis, G. E. Physics-informed neural networks: A deep learning framework for solving forward and inverse problems involving nonlinear partial differential equations. *Journal of Computational physics*, 378:686–707, 2019.
- Reynolds, O. On the dynamical theory of incompressible viscous fluids and the determination of the criterion. In *Proceedings of the Royal Society-Mathematical and Physical Sciences*, 1895.
- Rudy, S. H., Brunton, S. L., Proctor, J. L., and Kutz, J. N. Data-driven discovery of partial differential equations. *Science advances*, 3(4):e1602614, 2017.
- Schaeffer, H. Learning partial differential equations via data discovery and sparse optimization. *Proceedings of the Royal Society A: Mathematical, Physical and Engineering Sciences*, 473(2197):20160446, 2017.
- Strikwerda, J. C. *Finite difference schemes and partial differential equations*. SIAM, 2004.
- Takamoto, M., Praditia, T., Leiteritz, R., MacKinlay, D., Alesiani, F., Pflüger, D., and Niepert, M. Pdebench: An extensive benchmark for scientific machine learning. *arXiv preprint arXiv:2210.07182*, 2022.
- Wang, R. and Yu, R. Physics-guided deep learning for dynamical systems: A survey. *arXiv preprint arXiv:2107.01272*, 2021.
- Yang, T.-Y., Rosca, J. P., Narasimhan, K. R., and Ramadge, P. Learning physics constrained dynamics using autoencoders. In *Advances in Neural Information Processing Systems*, 2022.
- Zubov, K., McCarthy, Z., Ma, Y., Calisto, F., Pagliarino, V., Azeglio, S., Bottero, L., Luján, E., Sulzer, V., Bharambe, A., et al. Neuralpde: Automating physics-informed neural networks (pinns) with error approximations. *arXiv preprint arXiv:2107.09443*, 2021.
- Zwillinger, D. and Dobrushkin, V. *Handbook of differential equations*. Chapman and Hall/CRC, 1998.

## A. Experimental and implementation details

We provide further information regarding the experiments described in Section 4. We ran all of the experiments on a single standard GPU, and all training algorithms took  $< 10$  minutes to train. Full code implementation for creating the datasets and implementing PDEexplain and its baselines is available on [github.com/orilinia/PDEexplain](https://github.com/orilinia/PDEexplain).

To create the dataset, we generated signals using the `PyPDE` package. Each signal was generated with different initial conditions sampled from a Gaussian process posterior, and a-priori known Dirichlet boundary conditions  $u(x = 0) = u(x = L) = 0$ . As discussed in Section 2, we made an important change compared to other known methods: the PDE parameters  $(a, b, c)$  are uniformly sampled for each signal, instead of being constant, making the task much harder. In the constant coefficients experiment we generated the parameters from  $a \sim U[0, 2]$ ,  $b, c \sim U[-1, 1]$ . For the Burgers' equation dataset we used  $a \sim U[1, 2]$ .

### A.1. Implementation details

All algorithms described in this paper except for DI (i.e., PDEexplain, No-PDE and PDE-RHS) share the same context-extraction architecture. The architecture consists of an encoder-decoder network, both implemented as MLPs with 6 layers and 256 neurons in each layer. We found that concatenating the latent vector in the output of the encoder to the initial conditions of the signal  $u(t = 0)$  greatly improved results and convergence time, since it encourages the encoder to focus on the dynamics of the observed signal, rather than the initial conditions of it.

The second part of each algorithm uses the latent vector as an input to a Context-To-Dynamics network.

In PDEexplain we implemented this network as an MLP with 5 hidden layers, each with 1024 neurons. The output of the network is then the task-specific parameters with the correct shape. For the Burgers' equation for example, the output of the network is the parameter  $a$ , and a function  $b(u)$  with the same shape as  $u$ .

In the No-PDE algorithm, the Context-To-Dynamics network consumes the current PDE state and the latent vector, and outputs the PDE state in the next time step. The optimization function for this algorithm therefore tries to minimize the prediction error of  $u_{t+1}$  in addition to the autoencoder loss.

The PDE-RHS algorithm is similar to the PDEexplain algorithm as it tries to learn a derivative and not the predicted state. The Context-To-Dynamics network in this case consumes the latent vector and the current state, and outputs the right-hand-side of the PDE equation.

Both PDE-RHS and No-PDE baselines have the same architecture of the Context-To-Dynamics net as PDEexplain, and only differ in the shape of the output. Sharing the same architecture allow us to carefully compare these methods and answer the question of how mechanistic knowledge can be used.